Correlation between ultrasonic shear wave velocity and Poisson's ratio for isotropic porous materials

K. K. Phani

Abstract A new correlation between ultrasonic shear wave velocity and Poisson's ratio has been established for isotropic porous material based on physical acoustic theory. Poisson's ratio may decrease, increase or remain unchanged with decrease in shear wave velocity depending on pore-shape and Poisson's ratio of the bulk solid. In case of decreasing Poisson's ratio with decreasing shear wave velocity, it passes through a minimum and then increases again to reach a limiting value of 0.5. It has been further demonstrated that the Poisson's ratio versus porosity relation deduced from the proposed correlation agrees with the experimental data extremely well.

Introduction:

In a recent paper Kumar et al. [1] have reported that for isotropic solid materials Poisson's ratio decreases with increase in ultrasonic shear wave velocity and suggested a linear relationship between them. Based on Mori-Tanaka mean-field approach, Dunn and Ledbetter [2] have shown that for an isotropic porous solid, Poisson's ratio is a function of porosity, pore geometry, and Poisson's ratio, v_0, of the pore-free material. Their analysis shows that for materials with spherical pores and $v_0 > 0.2$, Poisson's ratio decreases with increasing porosity and for $v_0 < 0.2$ it increases with increase in porosity (refer to Fig. 1 of [2]) and remains constant for $v_0 = 0.2$. It is well established that ultrasonic shear wave velocities for porous ceramics and

metal powder compacts decrease with increasing porosity [3–6]. Therefore, for porous materials with spherical pores and $v_0 > 0.2$, Poisson's ratio will decrease with decrease in ultrasonic shear wave velocity and for $v_0 < 0.2$ it will increase with decrease in velocity. For the needle-shaped pores the variation of Poisson's ratio with porosity is qualitatively similar to those of the spherical pores [2] and therefore, a similar variation with ultrasonic shear wave velocity as those of spherical pores is expected. On the other hand, for materials with disk-shaped pores, Poisson's ratio decreases highly non-linearly with porosity [2] for any positive value of v_0 and increases with porosity for negative values of v_0. Negative Poisson's ratios are usually exhibited by highly anisotropic and foamed materials and we will not consider them in this analysis. Therefore for isotropic porous materials Poisson's ratios may either increase or decrease with ultrasonic shear wave velocities depending on the values of v_0 and pore geometry. Figure 1 shows a plot of Poisson's ratios of four different porous ceramic materials namely alumina [7], uranium dioxide [8], porcelain [9], reaction bonded silicon nitride (RBSN) [10], and silica gel [11] against their respective ultrasonic shear wave velocities. The straight lines fitted by regression analysis indicate the trends of variation of the data.[1] The Poisson's ratios, v_0, of these materials are 0.233, 0.316, 0.195, 0.201, and 0.159 for alumina, uranium dioxide, porcelain, RBSN, and silica gel respectively [7–11]. As expected from theory, Poisson's ratios decrease with shear wave velocities for alumina and uranium dioxide whereas those of porcelain and silica gel increase with velocities. However, the slopes of trend lines vary indicating possibly presence of pores of different geometries in these materials.

K. K. Phani (✉)
Central Glass & Ceramic Research Institute, Kolkata 700 032, India
e-mail: kkphani@cgcri.res.in

---

[1] Regression coefficients are 0.94, 0.93, 0.99, 0.80, and 0.40 for silica gel, porcelain, uranium dioxide, RBSN, and alumina, respectively.
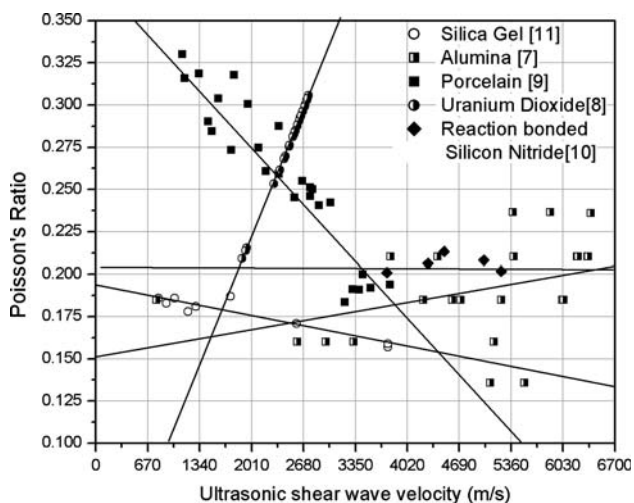
Fig. 1 Variation in Poisson's ratio with ultrasonic shear wave velocity for porous material with Poisson's ratio of bulk material greater, less, and equal to 0.2

For RBSN having $v_0 = 0.201$, it remains practically constant as predicted by the theory. Analysis given by Dunn and Ledbetter [2] also gives the limiting values of Poisson's ratios for different pore geometries as ultrasonic shear velocity approaches zero (i.e., as pore fraction approaches one). But as pointed out by them these limits are not valid since their model is not valid above a porosity of 40%. However, this limit can be deduced from the relation between Poisson's ratio and ultrasonic velocities given by the theory of physical acoustics [1], i.e.,

$$v = \frac{(V_L^2 - 2V_T^2)}{2(V_L^2 - V_T^2)} \quad (1)$$

where v is the Poisson's ratio and V_L and V_T are the ultrasonic longitudinal and shear velocities respectively. Equation 1 indicates that the limiting value of $v_0 = 0.5$ as V_T becomes zero. This predicts two interesting features of variation of Poisson's ratios with ultrasonic shear wave velocities for porous materials. For materials with $v < 0.2$ and having Poisson's ratio increasing with decrease in shear wave velocity, Poisson's ratio is expected to increase monotically and attain a value of 0.5 as V_T approaches zero. On the other hand, material having $v > 0.2$ and decreasing Poisson's ratio with decrease in shear velocity, it must pass through a minimum and increase again to satisfy Eq. 1 at $V_T = 0$.

In the present study, first a new correlation between Poisson's ratio and shear wave velocity is derived based on Eq. 1 and then a comparison between theory and experimental data is presented to analyze the interesting features of these variations.

Analytical derivation and data analysis

Equation 1 can be rearranged to express V_L as a function of V_T and v giving the relation

$$V_L^2 = V_T^2 \frac{2(1 - v)}{1 - 2v} \quad (2)$$

Assuming v can be expressed as a function of V_T (linear or otherwise) [1], Eq. 2 indicates that there exists a polynomial relationship between V_L and V_T. Therefore, we can write

$$V_L = f_1(V_T) \quad (3)$$

where $f_1(V_T)$ is a polynomial function of V_T. Equation 1 can now be used to express v in terms of V_T giving the relation

$$v = \frac{2 - [f(V_T)]^2}{2\left(1 - [f(V_T)]^2\right)} \quad (4)$$

where $f(V_T) = V_L/V_T = f_1(V_T)/V_T$ is a function of V_T only. It may be noted that if v remains invariant with ultrasonic velocity (or porosity), then Eq. 2 reduces to

$$V_L = \beta V_T \quad (5)$$

where β is a constant given by $\sqrt{\frac{2(1-v)}{(1-2v)}}$. In what follows an analysis of experimental data reported in the literature is presented in terms of Eqs. 1–5. These data sets include alumina [7, 12–15], uranium dioxide [8, 16], porcelain [9], silica gel [11] and reaction bonded silicon nitride [10]. Wherever velocity values have not been reported, they have been calculated from the reported values of Young's and shear moduli and density using the well-known relations given by the physical acoustics theory. The functional form of $f_1(V_T)$ is taken as

$$V_L = f_1(V_T) = \alpha + \beta V_T + \gamma V_T^2 \quad (6)$$

where α, β, and γ are constants. The values of these constants are evaluated considering ultrasonic velocity values at three points one of which is that of theoretically dense or pore-free material. Other two data points are taken from experimental values at two different porosities. The velocity values of theoretically dense or pore-free material are calculated from mean polycrystalline (VRH) values for elastic moduli wherever such data are available, otherwise the values for pore-free material as reported in the literature are used. Sum of squares, Q, is used as a measure of goodness of fit between data and Eq. 6. Q is given by
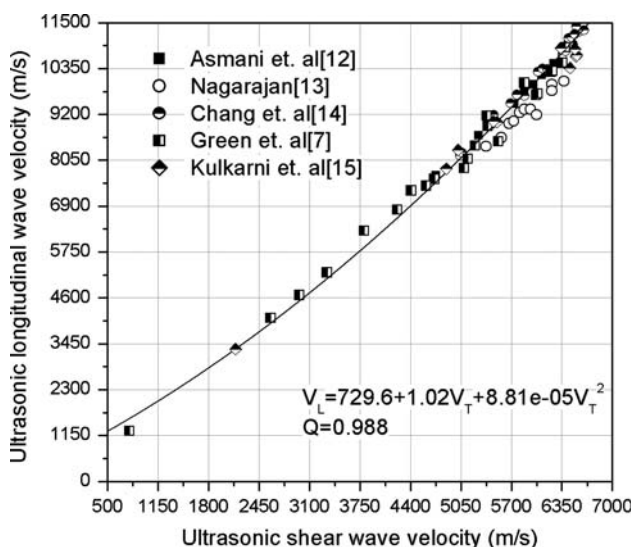
$$Q = 1 - \frac{\sum_{i=1}^{n} (V_{ci} - V_i)^2}{\sum_{i=1}^{n} (V_i - V_m)^2} \quad (7)$$

where V_{ci} is the calculated i-th value from the fitted equation, V_i is the measured value, V_m is the mean of the measured values, and n is number of data points. For values of Q > 0.95 the fit is considered to be good.

Alumina

In Fig. 2 experimental values of ultrasonic longitudinal velocities, V_L, have been plotted against ultrasonic shear velocities, V_T, for alumina reported by various researchers [7, 12–15]. Within the limits of experimental errors all the data points seem to fall on a single curve even though various methods of fabrication have been adopted by these researchers namely uniaxial pressing [12, 13], uniaxial pressing followed by isostatic pressing [7], pressure casting of colloidal slurry [14], and slip casting [15]. Different methods of fabrication are likely to give different pore geometries and it is well established now that besides porosity, different pore geometries also affect ultrasonic velocities differently [17]. Therefore, the observation that all the data points fall on a single curve possibly indicate that pore geometry affects both longitudinal velocity and shear velocity in identical manner. Values of α, β, and γ in Eq. 6 were evaluated using pore-free longitudinal and shear wave velocities of alumina as 10839.0 m/s and 6399.4 m/s, respectively calculated from mean polycrystalline elastic properties as reported by Anderson et al. [18] and the experimentally determined velocity values corresponding to porosities of 36.6% and 17.8% as reported by Kulkarni et al. [15] giving the relation

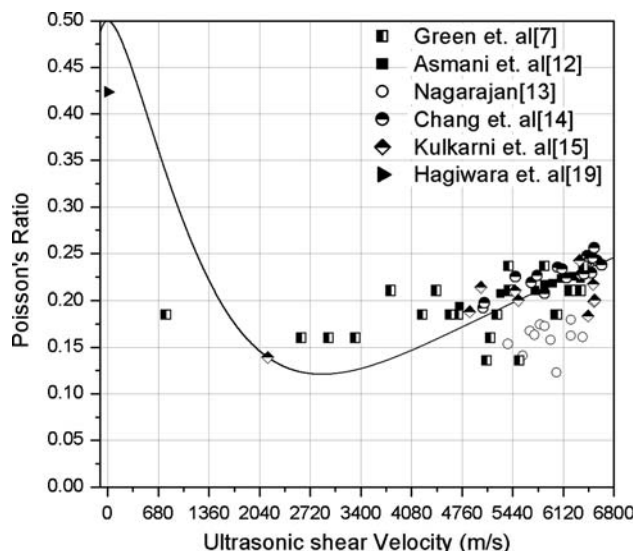$$V_L = 729.6 + 1.0V_T + 8.81 \times 10^{-5} V_T^2 \tag{8}$$

with a value of Q = 0.988. Equation 8 is also plotted in Fig. 2 and it agrees with the data well. Equation 4 with $f(V_T)$ values derived from Eq. 8 is plotted in Fig. 3 along with the experimental values of Poisson's ratio calculated from the measured velocity values. Considering the fact that Poisson's ratio is more sensitive to the error of measurements, the predicted values show reasonable agreement with the data. Since the value of Poisson's ratio of pore-free alumina is 0.233, it initially decreases with velocity, as expected. The minimum value of Poisson's ratio is reached at a shear velocity of 2,720 m/s and then it increases again. Unfortunately very few data points are available to confirm this increasing trend. To further confirm this increasing trend, a value of the Poisson's ratio for foamed alumina as reported by Hagiwara et al. [19] has also been plotted in Fig. 3. It seems to agree with the trend predicted by Eq. 4 quite well.
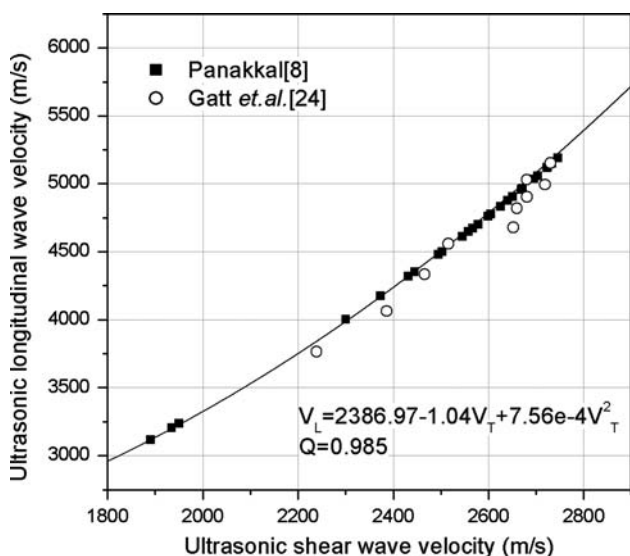
Uranium dioxide

Figure 4 shows ultrasonic longitudinal wave velocity of sintered uranium dioxide plotted against ultrasonic shear wave velocity as reported by Panakkal [8]. Again values of α, β, and γ were evaluated using longitudinal and shear wave velocities of pore-free uranium dioxide as 5469.0 m/s and 2823.9 m/s, respectively, calculated from mean polycrystalline elastic properties as reported by Wachtman et al. [20] and the experimentally determined velocity values corresponding to porosities of 20.0% and 12.5% as reported by Panakkal [8] yielding the relation

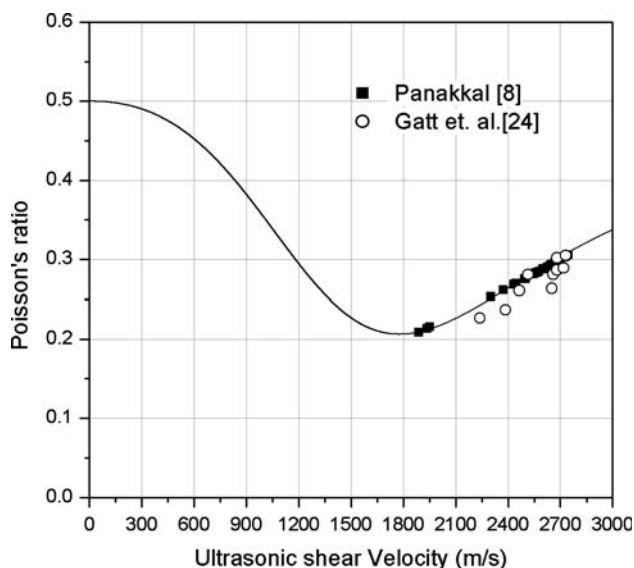$$V_L = 2386.97 - 1.04V_T + 7.56 \times 10^{-4}V_T^2 \tag{9}$$

Fig. 2 Variation of ultrasonic longitudinal velocity with ultrasonic shear wave velocity of Alumina as reported by different researchers

Fig. 3 Variation of Poisson's ratio of porous alumina with ultrasonic shear wave velocity

Fig. 4 Variation of ultrasonic longitudinal velocity with ultrasonic shear wave velocity of uranium dioxide as reported by different researchers

with $Q = 0.985$. It may be mentioned that the data reported by Panakkal [8] is the collection of data reported by four different researchers [20–22] including his own [16, 23], yet the two ultrasonic velocities show excellent close correlation confirming again that pore geometry affects longitudinal and shear wave velocities identically. Also plotted in Fig. 4 are data of ultrasonic velocities reported by Gatt et al. [24]. As before, these values agree closely with the fitted Eq. 9 as indicated by a value of $Q = 0.985$.

Figure 5 shows the variation of Poisson's ratio with shear wave velocity, calculated from Eq. 4 along with

Eq. 9. Also plotted in Fig. 5 are the Poisson's ratios as reported by Panakkal [8] and Gatt et al. [24] showing excellent agreement with the predicted values. Poisson's ratio values were calculated from the measured velocity data. Since the Poisson's ratio of dense uranium dioxide is 0.316 [20], it initially decreases with velocity and then increases after reaching a minimum value at a velocity of 1,700 m/s.
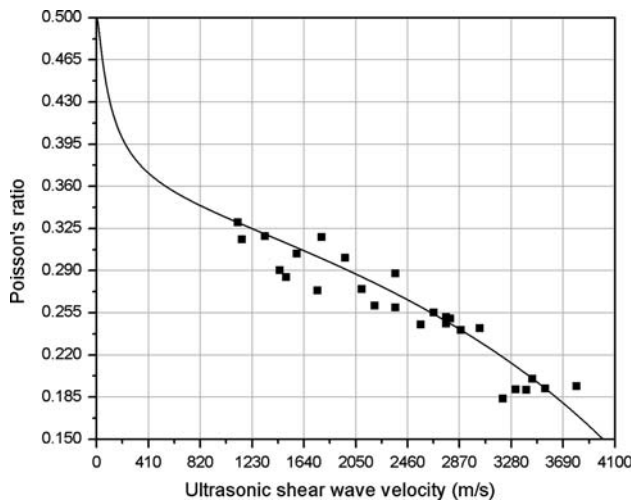
Porcelain

Ultrasonic wave velocities of porcelain as reported by Boisson et al. [9] are shown in Fig. 6. Since measured velocity values of pore-free material were not available, values of α, β, and γ were evaluated using experimentally measured velocity values at porosities of 10.8, 17, and 37%. Here again, longitudinal wave velocities show a close correlation with shear wave velocities giving the relation

$$V_L = 85.72 + 2.05\ V_T - 1.29 \times 10^{-4}\ V_T^2 \tag{10}$$

with a value of $Q = 0.998$. In Fig. 7 experimental Poisson's ratio values, calculated from measured velocity values, have been plotted against shear wave velocities along the predicted values calculated from Eq. 4 and the fitted Eq. 10. Predicted values agree with the experimental data quite well. Poisson's ratio of pore-free porcelain is estimated to be 0.195 from the values of ultrasonic velocities of pore-free material estimated by Roth et al. [3]. Since v_0 is less than 0.2, Poisson's ratio shows an increasing trend with decreasing velocity as predicted by the theory.

Fig. 5 Variation of Poisson's ratio of porous uranium dioxide with ultrasonic shear wave velocity
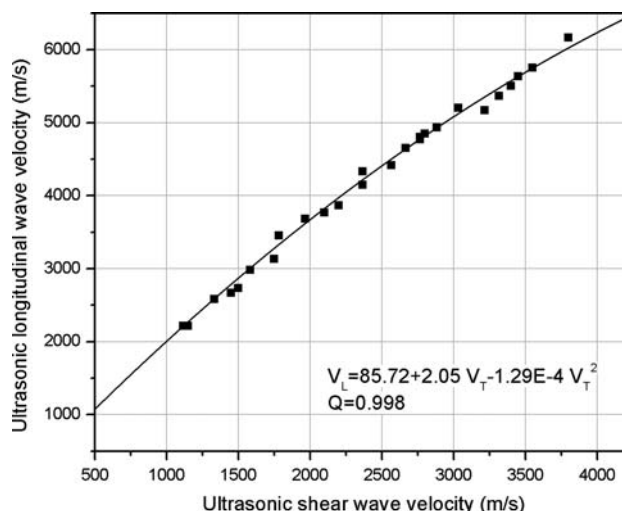
Fig. 6 Variation of ultrasonic longitudinal velocity with ultrasonic shear wave velocity of Porcelain

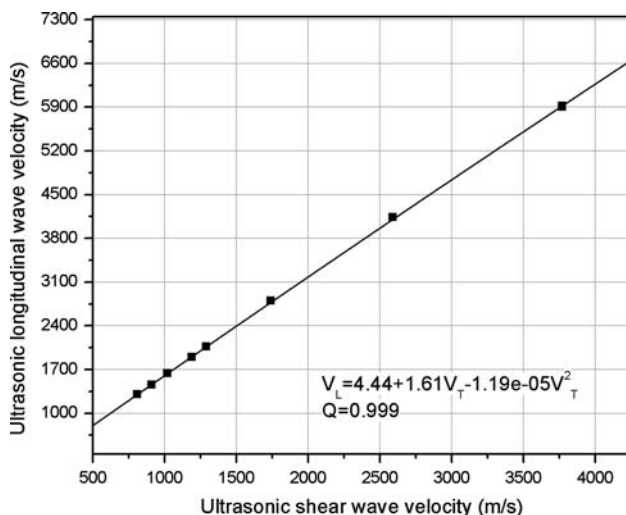**Fig. 7** Variation of Poisson's ratio of porcelain with ultrasonic shear wave velocity
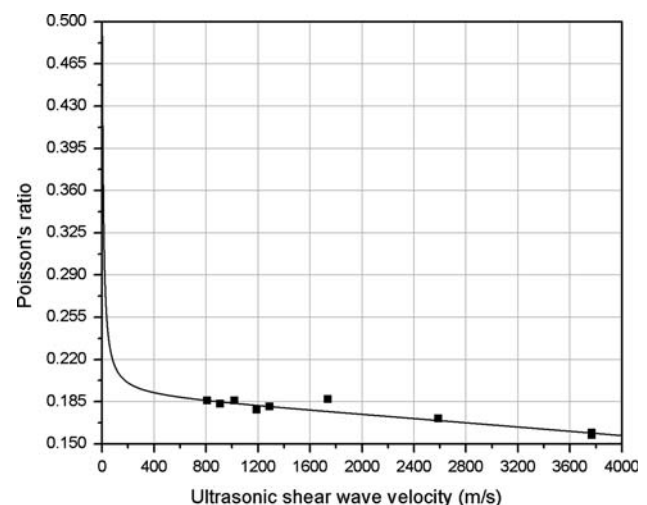
variation of Poisson's ratio with shear wave velocity as calculated from Eqs. 4 and 11 along with the experimental data of Poisson's ratio calculated from measured velocities [11]. The experimental data agree with the predicted values extremely well. Poisson's ratio of pore-free silica gel has been reported by Adachi and Sakka [11] as 0.159 and therefore, as expected from theory Poisson's ratio increases with decrease in shear wave velocity. As can be seen from Fig. 9, Poisson's ratio increases sharply below a shear wave velocity of 800 m/s. Unfortunately the data reported by Adachi and Sakka [11] cover a range of shear wave velocity up to 800 m/s only. A further confirmation regarding this nature of variation is given later based on the data of Ashkin et al. [27] for colloidal gel-derived silica having ribbon-like pore structure.

Silica gel

Figure 8 shows a plot of ultrasonic velocities of silica gel reported by Adachi and Sakka [11]. They prepared silica gel by sol–gel method from a tetramethoxysilane solution with porosity varying in the range 0–0.726. The longitudinal velocity values have been calculated from their reported values of shear wave velocities and Poisson's ratios using Eq. 2. The values α, β, and γ were evaluated using experimentally measured velocity values for pore-free material and for porosities of 72.6 and 38.9% giving the relation

$$V_L = 4.44 + 1.61V_T - 1.19 \times 10^{-5} \, V_T^2 \tag{11}$$

with Q = 0.999 showing excellent agreement between the data and the fitted equation. Figure 9 shows the predicted
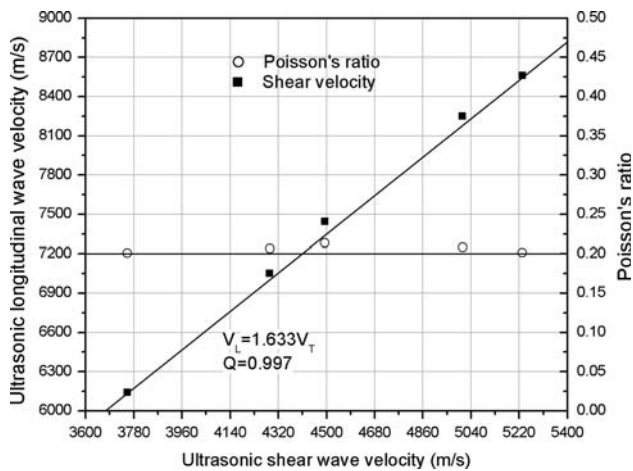
RBSN

In Fig. 10 Poisson's ratios and longitudinal wave velocities of RBSN as reported by Thorp and Bushell [10] have been plotted against shear wave velocities. As can be seen from Fig. 10 Poisson's ratio remains constant at a value of 0.2 with the change in shear wave velocities. Therefore the variation in longitudinal wave velocities with shear wave velocities is given by Eq. 5 with the value of $\beta = 1.633$ for $v_0 = 0.2$, i.e.,

$$V_L = 1.633V_T \tag{12}$$

Equation 12 is also plotted in Fig. 10. It shows an excellent agreement with the velocity data having a value of Q = 0.997.

Fig. 8 Variation of ultrasonic longitudinal velocity with ultrasonic shear wave velocity of Silica gel prepared by sol–gel method

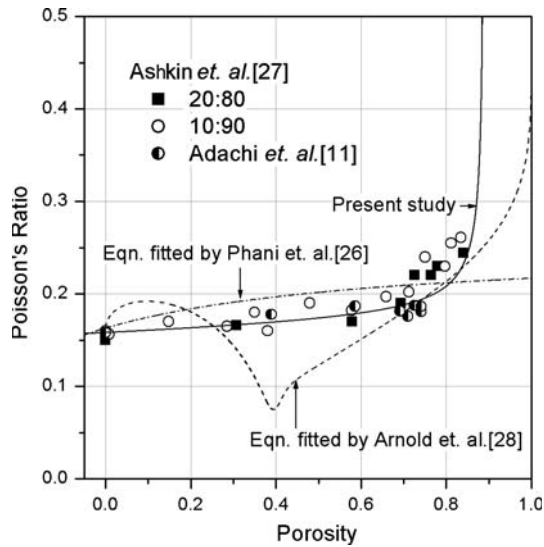**Fig. 9** Variation of Poisson's ratio of silica gel with ultrasonic shear wave velocity

Fig. 10 Variation of ultrasonic longitudinal wave velocity and Poisson's ratio of RBSN with ultrasonic shear wave velocity

Discussion

The analysis of experimental data as presented in the previous section shows that for isotropic porous materials, the variation of Poisson's ratio with ultrasonic shear wave velocity is in agreement with the theoretically predicted trends based on Mori-Tanaka mean-field approach [2]. Poisson's ratio may initially increase, decrease, or remain unchanged with decrease in shear wave velocity depending on the pore shape and Poisson's ratio of the bulk solid. In case of decreasing Poisson's ratio with shear wave velocity, it passes through a minimum and then increases again to satisfy the limiting condition $v = 0.5$ at $V_T = 0$, as imposed by the physical acoustics theory. The experimental data on alumina and uranium dioxide having $v_0 > 0.2$, analyzed earlier, show this behavior. However, the rate of decrease of Poisson's ratio with decrease in shear wave velocity is higher in case of uranium dioxide compared to that of alumina (refer to Figs. 3 and 5). This is attributed to the different pore structure of these two materials. According to the analysis given by Dunn and Ledbetter [2], the rate of decrease or increase of Poisson's ratio with porosity is dependent on pore geometry and it is in the order—disk shape > needle shape > spherical shape—with minimum increase or decrease for spherical shape pores. Therefore, from the nature of variation as shown in Figs. 3 and 5, it may be inferred that the pore geometry in case of uranium dioxide can possibly be described by disk-shaped pores whereas that of alumina by either needle-shaped or spherical pores. This observation agrees well with the analysis of data on uranium dioxide (shown in Fig. 5) made by Gatt et al. [24] based on numerical simulation. They have concluded that inter-granular pores in uranium dioxide have ellipsoidal shapes and their aspect ratio is lower than about 0.25

(penny-shaped oblates). Phani [25] has also shown that elastic properties of alumina as reported by Nagarajan [13] can be well described by using a cylindrical pore model.

For both porcelain and silica gel having $v_0 < 0.2$ Poisson's ratio increases with decrease in shear wave velocity. As mentioned earlier, with disk-shaped pores, Poisson's ratio decreases highly nonlinearly with increasing porosity and hence with decreasing shear wave velocity for any positive value of v_0. Therefore, increasing values of Poisson's ratios with decreasing shear wave velocities in case of porcelain and silica gel rule out the possibility of disk-shaped pores in these materials. On the other hand, for any material having $v_0 < 0.2$, if the Poisson's ratio decreases with decrease in the shear wave velocity, it will indicate presence of pores in the shape of thin disks only. Thus from the theoretical analysis it will be only logical to assign needle-shaped pores to porcelain which shows higher rate of increase in Poisson's ratio with decreasing shear wave velocity compared to that of silica gel and assume that pores in silica gel are spherical in shape. However, in an earlier study Phani and Sanyal [26] have shown that silica gel as prepared by Adachi and Sakka [11] by sol–gel method has a ribbon-like pore structure similar to that of colloidal gel-derived silica as reported by Ashkin et al. [27]. This has been established by comparing Young's modulus versus porosity data reported by these two researchers. Fig. 12 shows the variation of Poisson's ratio with porosity of colloidal gel-derived silica as reported by Ashkin et al. [27] along with the values of sol–gel-derived silica given by Adachi and Sakka [11]. The similar variation of Poisson's ratio with porosity for these two data sets, again confirms the similarity of their pore structure. Arnold et al. [28] have analyzed this data set assuming pores to be spherical and observed that the Poisson's ratio versus porosity relation is concave downward up to a porosity value of 0.4 and is convex upward above this value giving a distinct kink at a porosity of 0.4. Their fitted equation is shown in Fig. 11. Phani and Sanyal [26] have shown that such a sharp transition in Poisson's ratio with porosity is an outcome of data analysis procedure and does not indicate the true nature of the variation. They analyzed the data assuming a ribbon-like pore structure and the equation fitted by them is also shown in Fig. 11. The fitted equation agrees with the data well but it fails to explain the sharp increase in Poisson's ratio above a porosity of 0.7. To reanalyze the data in terms of Eq. 4, proposed in this study, we need to express Eq. 4 in terms of porosity and for this, variation of V_T with porosity must be known. Unfortunately, Ashkin et al. [27] have neither reported shear wave velocity nor shear modulus for the material studied by them. Therefore, to express the variation of V_T with porosity, p, the data reported by Adachi and Sakka [11] is utilized. These data are shown in Fig. 12.

Fig. 11 Variation of Poisson's ratio of colloidal gel-derived silica with porosity
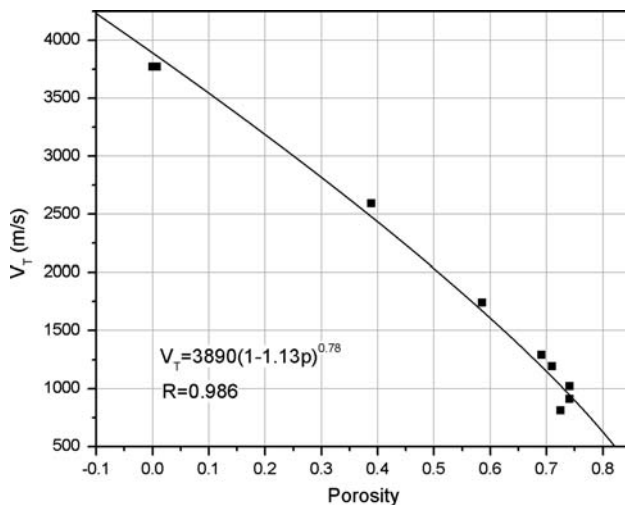
Fig. 12 Variation of ultrasonic shear wave velocity of silica gel prepared by sol–gel method, with porosity

A power law equation as suggested by Phani and Maitra [29] is fitted to the data taking the shear wave velocity of pore-free silica gel as 3,890 m/s [11] giving the relation

$$V_T = 3890 \, (1 - 1.13\mathrm{p})^{0.78} \qquad (13)$$

with a coefficient of correlation of 0.986. Equation 13 has also been plotted in Fig. 12.

Equations 4, 11, and 13 can be used together to describe the variation of Poisson's ratio with porosity for silica gel. The predicted variation is shown in Fig. 11 (solid line). The agreement between the predicted values and the experimental data speaks for itself. This also confirms the sharp increase in Poisson's ratio of silica gel below a shear

wave velocity of 800 m/s (or above a porosity of 0.7) as shown in Fig. 9 and the ribbon-like pore structure of the silica gel prepared by Adachi and Sakka [11] by sol–gel method. This leaves one question unanswered—what is the pore structure of porcelain? In absence of microstructural details this issue cannot be resolved.

Finally it may be mentioned that the above inferences regarding pore structure have been made based on the analysis of Dunn and Ledbetter [2]. However, in absence of detailed microstructure of the materials analyzed here (except for the data reported by Ashkin et al. [27]) these cannot be confirmed.

Conclusions

The variation of Poisson's ratio of isotropic porous material with ultrasonic shear wave velocity has been studied and a new correlation has been proposed to describe its variation with shear wave velocity based on the theory of physical acoustics. The study indicates that

1. for isotropic porous materials ultrasonic longitudinal velocity is closely related to ultrasonic shear wave velocity irrespective of the pore structure of the material; indicating that the pore geometry affects both longitudinal velocity and shear velocity in identical manner.
2. for materials having spherical and needle-shaped pores and Poisson's ratio of bulk material greater than 0.2, Poisson's ratio initially decreases with decrease in shear wave velocity and goes through a minimum and then increases with decrease in velocity reaching a limiting value of Poisson's ratio of 0.5. On the other hand, for bulk material Poisson's ratio less than 0.2, Poisson's ratio monotonically increases with decrease in velocity with a limiting value of 0.5 for Poisson's ratio.
3. for disk-shaped pores Poisson's ratio decreases with shear wave velocity for any value of Poisson's ratio of bulk material greater than zero, passes through a minimum value and then increases with decrease in velocity. This also indicates that if Poisson's ratio decreases with decreasing shear wave velocity for any material having Poisson's ratio of bulk material less than 0.2, the material will have pores in the shape of disks.
4. for materials having needle or spherical-shaped pores and Poisson's ratio of bulk material equal to 0.2, Poisson's ratio remains constant with change in shear wave velocity.
5. variation of Poisson's ratio with shear wave is in general agreement with the predictions based on Mori-Tanaka mean-field approach.

6. Poisson's ratio versus porosity relation deduced from the new correlation correctly predicts the increasing trend of Poisson's ratio with porosity for materials having ribbon-shaped pores.

References

1. Kumar A, Jayakumar T, Raj B, Ray KK (2003) Acta Mater 51:2417
2. Dunn ML, Ledbetter H (1995) J Mater Res 10:2715
3. Roth DJ, Stang DB, Swickward SM, DeGuire MR (1990) NASA Technical Memorandum 102501
4. Yeheskel O, Shokhat M, Ratzker M, Dariel P (2001) J Mater Sci 36:1219
5. Panakkal JP, Willems H, Arnold W (1990) J Mater Sci 25:1397
6. Martin LP, Dadon D, Rosen M (1996) J Am Ceram Soc 79:1281
7. Green DJ, Nader C, Brezny R (1990) Ceram Trans 7345
8. Panakkal JP (1991) IEEE Trans Ferroelec Freq Control 38:161
9. Boisson J, Platon F, Boch P (1976) Ceramurgia 674
10. Thorp JS, Bushell TG (1985) J Mater Sci 20:2265
11. Adachi T, Sakka S (1990) J Mater Sci 25:4732
12. Asmani M, Kermel C, Leriche A, Ourak M (2001) J Eur Ceram Soc 21:1081
13. Nagarajan A (1971) J Appl Phys 42:3693
14. Chang LS, Chuang TS, Wei WJ (2000) Mater Char 45:221
15. Kulkarni N, Moudgil B, Bhardwaj M (1994) Am Ceram Soc Bull 73:146
16. Panakkal JP, Ghosh JK (1984) J Mat Sci Lett 3:935
17. Rice RW (1998) Porosity in Ceramics. Marcel Dekker Inc., New York
18. Anderson OL, Schreiber E, Lieberman RC, Soga N (1968) Rev Geophys 6:491
19. Hagiwara H, Green DJ (1987) J Am Ceram Soc 70:811
20. Wachtman JB, Wheat ML, Anderson HJ, Bates JL (1965) J Nucl Mater 16:39
21. Padel A, Novion CD (1969) J Nucl Mater 33:40
22. Boocock J, Furzer AS, Matthews JR (1972) AERE Rep. No. M 2565
23. Panakkal JP, Ghosh JK, Roy PR (1984) J Phys D: Appl Phys 17:1791
24. Gatt J-M, Monerie Y, Laux D, Baron D (2005) J Nucl Mater 336:145
25. Phani KK (1996) J Mater Sci 31:262
26. Phani KK, Sanyal D (2005) J Mater Sci 40:5685
27. Ashkin D, Haber RA, Wachtman JB (1990) J Am Ceram Soc 73:3376
28. Arnold M, Boccaccini AR, Ondracek G (1996) J Mater Sci 31:1643
29. Phani KK, Maitra AK (1994) J Mater Sci 29:4415